Optimal Tuning of PI Controllers for DFIG-Based Wind Energy System using Self-adaptive Differential Evolution Algorithm

Hemanth Kumar Raju Alluri[1], Ayyarao SLV Tummala[2], Ramanarao PV[3], and PVN Mohan Krishna[1]

[1] Department of Electrical & Electronics Engineering, SRKREC, Bhimavaram, India.
[2] Department of Electrical & Electronics Engineering, GMRIT, Rajam, India.
[3] Department of Electrical & Electronics Engineering, ANU, Guntur, India.

Abstract: The rapid infiltration of wind energy systems in the power system is causing huge power fluctuations due to varying wind speeds and fault occurrences. Here objective is to tune the Proportional Integral (PI) controller parameters. Formulation of objective function with Integral Square Error (ISE) concept is to minimize the errors of active power, terminal voltage and DC bus voltage. To tune these control parameters a Self-adaptive Differential Evolution (SaDE) approach is adopted. These optimized parameters are applied to a 9 MW wind generation system using Doubly-Fed Induction Generator's (DFIG) and compared this system with the actual system in MATLAB/Simulink. The results obtained here are found to be superior in terms of settling time, peak overshoot and undershoots, voltage profile.

Keywords: Vector control of DFIG, PI control parameters, Formulation of Objective function, Self - adaptive Differential Evolution, Fault analysis.

1. Introduction

Present fossil fuels supply major part of world's energy. There is a serious concern over use of fossil fuels, as they lead to global climate change. The usage of fossil fuels leads to serious environmental aspects. When these fuels were burnt, they emit carbon-dioxide (CO_2) which induces heat in atmosphere leads to global warming. Over the last few years, there has been a strong penetration of renewable energy resources into the power network. Wind generation has played and will continue to play an important role in smart grid for coming years. Wind energy is popular because of the advantages like pollution free, less space for installation, price stability, job creation, etc[1]. The potential of wind energy is very higher than what the entire human needs. To gear the critical challenges, major efforts are taking in this area in various levels of research works.

DFIG's are mostly used in wind energy system rather than Squirrel-cage induction generator, Wound-rotor induction generator and Permanent magnet synchronous generator because of various advantages like active and reactive power controllability, low converter size, less mechanical stress, smooth grid connection, lower losses and compact size[2]. DFIG operates in both Sub-synchronous and Super-synchronous generating modes, which varies according to the wind speed[3]. In wind power systems the DFIG's stator is directly connects to grid and rotor is connected to grid through the back to back converters with IGBT based Pulse Width Modulation converters. The converters are controlled by using Rotor Side Controller (RSC) and Grid Side Controller (GSC) and DC link capacitor is placed between the converters which are shown in Figure 1. The controller controls the RSC and GSC converters to gain optimal power control and stability of power system. Independent active and reactive power control is achieved using Vector Control of DFIG[4]. Vector control of DFIG operates with two PI controllers in power control loop and two PI controllers in reactive power control loop.

Many nonlinear control techniques like sliding mode control[5], Feedback linearization control[6], decentralized non-linear control[7], etc. are proposed in the literature. But the design of these controls is complex and there is no evidence of implementation in practice. Therefore

Received: November 10th, 2018. Accepted: June 23rd, 2019
DOI: 10.15676/ijeei.2019.11.2.9

the major challenge in wind energy based DFIG system is selection of optimum PI control parameters that improves system performance and stability.

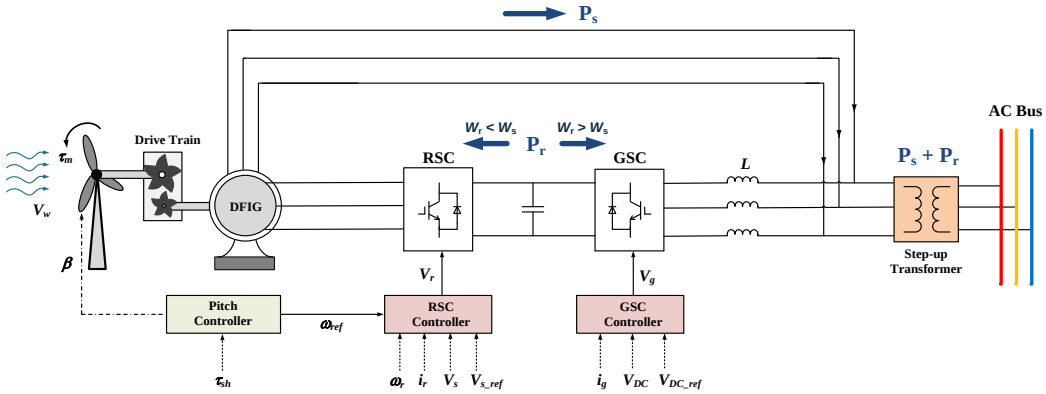

Figure 1. Schematic of Wind system with DFIG

The parameters of the PI controller can be tuned using Ziegler-Nichols method[8], Kappa-tau tuning[9], Pole placement technique etc. But the recent trend is tuning the PI controller parameters using advanced optimization techniques. One of the recent developed optimization techniques is Differential evolution (DE). Basic version of DE is proposed by Storn and Price[10]. Because of its simplicity in concept and implementation, there are many applications of DE like tuning of PI controller, tuning of extended kalman filter[11], etc. The effectiveness, efficacy and robustness of DE depend on the selection of suitable mutation strategy and optimum scaling factor α, cross-overrate C_R values. This requires high computation time and rigorous decision making. Therefore several modified versions of DE like Opposition based Differential Evolution, Differential Evolution using a neighborhood-based mutation operator[12], Composite Differential Evolution (CoDE)[13], jDE, etc. are proposed. SaDE is one of the modified versions of DE and it is proposed by Qin and Suganthan[14]. In this algorithm Self-adaption of the parameters and learning strategies are done during evolution by learning experience of algorithm. SaDE algorithm is best compared to DESAP and FADE. Several optimization techniques like Particle Swarm Optimization (PSO)[15], Genetic Algorithm (GA)[16], Differential Evolution (DE)[17], bacteria foraging[18] are proposed in the literature to tune the parameters of PI controller to Wind based DFIG system. The performance of the system can be enhanced by adopting SaDE.

The objective of this paper is to tune the parameters of PI controllers using SaDE. The objective function is formulated so that active power and terminal voltage tracks the reference values with less peak overshoot and settling time. The parameters are tuned for 9 MW wind farm with six turbines each having a capacity of 1.5 MW. The performance of SaDE tuned system is compared with actual system.

The remaining part of the paper is organized in various sections. Where, Section 2 presents the dynamic model of wind system with DFIGURE Section 3 describes tuning of PI controller parameters using SaDE technique. In Section 4 simulations are carried out. Finally, we conclude the paper in the last section.

2. Dynamic model of Wind system using DFIG

In wind power system as shown in Figure 1, wind turbine is coupled to the gear box mechanism, which is having various low and high speed shafts to drive the DFIG with rated speed. The controllers are used to produce smooth grid connection of parameters like voltage and frequency even in sub-synchronous and super-synchronous generating modes of operation.

A. Modeling Drive Train:

The drive train system plays an important role to drive DFIGURE The model is represented in (1-3);

$$\frac{d\omega_t}{dt} = \frac{1}{2H_t}(T_m - T_{sh}) \quad (1)$$

$$\frac{d\theta_{tw}}{dt} = \omega_t - (1 - s_r)\omega_s \quad (2)$$

$$\frac{ds_r}{dt} = \frac{-1}{2H_g\omega_s}[T_{em} + T_{sh}] \quad (3)$$

Parameters;

$\omega_t \rightarrow$ Angular speed of turbine

$H_t \rightarrow$ Turbine's inertia constant

$T_m \rightarrow$ Wind turbine torque

$T_{sh} \rightarrow$ Shaft torque

$\theta_{tw} \rightarrow$ Twist angle of shaft

$H_g \rightarrow$Generator's inertia constant

$T_{em} \rightarrow$ Electromagnetic torque

$s_r \rightarrow$ Slip of the rotor

$\omega_s \rightarrow$ Angular synchronous speed

B. Modeling of Pitch control

Pitch angle is used for controlling the output power of system at high winds. To avoid complexity, pitch angle reference is taken as zero at wind speed is reduced from the rated speed. In case if wind speed exceeds the rated speed then pitch controller will adjust the pitch angle to avoid overflow of power.

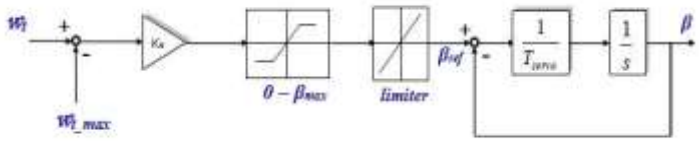

Figure 2. Block diagram of pitch controller

Block diagram of pitch controller is shown in Figure 2. This pitch control is modeled by using the modeling equation refer to (4),

$$\frac{d\beta}{dt} = \frac{1}{T_\beta}(\beta_{ref} - \beta) \quad (4)$$

Parameters;

$\beta \rightarrow$ Pitch angle

$\beta_{ref} \rightarrow$ Reference pitch angle

C. Modeling of DFIG

Every machine can be modeled in two-pole machine model. Here DFIG is expressed in d-q reference frame. The differential equations of the stator currents and voltage equations are given in (5), (6), (7) and (8);

$$\frac{dE_d^{'}}{dt} = s_r\omega_s E_q^{'} - \omega_s \frac{L_m}{L_{rr}} u_{qr} - \frac{1}{T_0^{'}}\left[E_d^{'} + (X_s - X_s^{'})i_{qs}\right] \quad (5)$$

$$\frac{dE_q^{'}}{dt} = -s_r\omega_s E_d^{'} + \omega_s \frac{L_m}{L_{rr}} u_{dr} - \frac{1}{T_0^{'}}\left[E_q^{'} - (X_s - X_s^{'})i_{ds}\right] \quad (6)$$

$$\frac{di_{ds}}{dt} = \frac{\omega_s}{X_s^{'}}\left\{u_{ds} - \left[R_s + \frac{1}{\omega_s T_0^{'}}(X_s - X_s^{'})\right] i_{ds} - (1 - s_r)E_d^{'} - \frac{L_m}{L_{rr}} u_{dr}\right\} + \frac{1}{X_s^{'} T_0^{'}} E_q^{'} + \omega_s i_{qs} \quad (7)$$

$$\frac{di_{qs}}{dt} = \frac{\omega_s}{X_s^{'}}\left\{u_{qs} - \left[R_s + \frac{1}{\omega_s T_0^{'}}(X_s - X_s^{'})\right] i_{qs} - (1 - s_r)E_q^{'} - \frac{L_m}{L_{rr}} u_{qr}\right\} - \frac{1}{X_s^{'} T_0^{'}} E_d^{'} - \omega_s i_{ds} \quad (8)$$

Parameters;

$E_d^{'} \rightarrow$ Voltage behind transient reactance on d-axis

$E_q^{'} \rightarrow$ Voltage behind transient reactance on q-axis

$i_s \rightarrow$ Current through stator

$L_{ss} \rightarrow$ Self-inductance of stator

$L_{rr} \rightarrow$ Self-inductance of rotor

$L_m \rightarrow$ Mutual inductance

$T_0^{'} \rightarrow$ Time constant of rotor's circuit

$u_s \rightarrow$ Terminal voltage of stator

$u_r \rightarrow$ Terminal voltage of rotor

$R_s \rightarrow$ Resistance of the stator

$X_s \rightarrow$ Reactance of the stator

$X_s^{'} \rightarrow$ Transient reactance of stator

D. Modeling of RSC

The Rotor side controller controls the terminal voltage (u_s) and output active power (P) by using i_{qr} and i_{dr} as shown in Figure 3. By employing two nested PI controllers, we can control the active power and terminal voltage by using Intermediate variables.

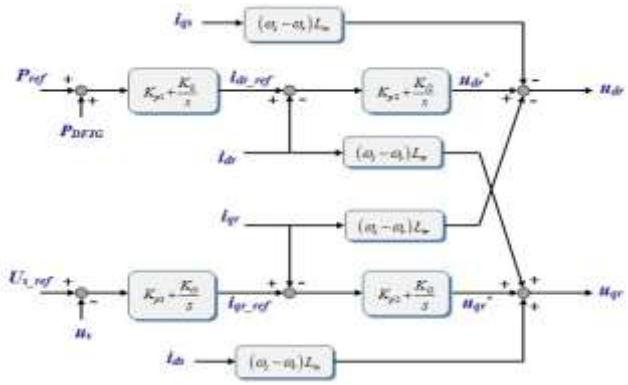

Figure 3. Block diagram of Rotor Side Converter controller

The control mechanism of Rotor Side Controller is shown in Figure 3. Based on this block diagram of RSC controller, the controlling equations are in (9), (10), (11) and (12);

$$\frac{dx_1}{dt} = P_{ref} + P_s + P_g \quad (9)$$

$$\frac{dx_2}{dt} = K_{p1}\left(P_{ref} + P_s + P_g\right) + K_{i1}x_1 - i_{dr} \quad (10)$$

$$\frac{dx_3}{dt} = u_{s\_ref} - u_s \quad (11)$$

$$\frac{dx_4}{dt} = K_{p3}\left(u_{s\_ref} - u_s\right) + K_{i3}x_3 - i_{qr} \quad (12)$$

Parameters;

$x_1 \quad x_2 \quad x_3 \quad x_4 \rightarrow$ Intermediate Variables

$K_{p1} \quad K_{i1} \rightarrow$ Power regulator gains

$K_{p2} \quad K_{i2} \rightarrow$ RSC current regulator gains

$K_{p3} \quad K_{i3} \rightarrow$ Voltage of grid side regulator gains

$i_r \rightarrow$ Current through rotor

$P_s \rightarrow$ Active power of the stator

$P_g \rightarrow$ Active power of GSC converter

$P_{ref} \rightarrow$ Reference active power of DFIG

$P_B \rightarrow$ Max active power at base turbine speed

$\omega_{tB} \rightarrow$ Base turbine speed

E. Modeling of DC link

The balancing of active power energy is done by this DC link capacitor. The balance is represented with

$P_r = P_g + P_{DC}$

Then the equation is given by;

$$P_r = u_{dr} i_{dr} + u_{qr} i_{qr}$$

$$P_g = u_{dg} i_{dg} + u_{qg} i_{qg}$$

$$P_{DC} = u_{DC} i_{DC} = -C u_{DC} \frac{du_{DC}}{dt}$$

By substituting the above terms into (13),

$$C u_{DC} \frac{du_{DC}}{dt} = u_{dg} i_{dg} + u_{qg} i_{qg} - \left(u_{dr} i_{dr} + u_{qr} i_{qr}\right) \quad (13)$$

Where;

$$u_{dg} = K_{p5}\left(-K_{p4} \Delta u_{DC} + K_{i4} x_5 - i_{dg}\right) + K_{i5} x_6 + X_{Tg} i_{qg} + u_{ds}$$

$$u_{qg} = K_{p5}\left(i_{qg\_ref} - i_{qg}\right) + K_{i5} x_7 + X_{Tg} i_{dg} + u_{qs}$$

Parameters;

$P_r \rightarrow$ Active power of the rotor side converter

$u_g \rightarrow$ Grid side converter voltage

$i_g \rightarrow$ Current through grid side converter

$P_{DC} \rightarrow$ Instant active power into DC link

$u_{DC} \rightarrow$ DC link capacitor voltage

$i_{DC} \rightarrow$ Current through capacitor

$C \rightarrow$ Capacitance

$X_{Tg} \rightarrow$ Reactance of fed-back transformer

$i_{qg\_ref} \rightarrow$ Reference of q-axis on grid side converter

F. Modeling of GSC

The Grid side controller controls the Reactive power and DC link voltage (u_{DC}) by using i_{qg} and i_{dg} as shown in Figure 4. By employing two series PI controllers, we can control the reactive power and DC link voltage by using Intermediate variables.

The control mechanism of Grid Side Controller is shown in Figure 4. Based on this block diagram of GSC controller, the controlling equations are presented in (14), (15) and (16);

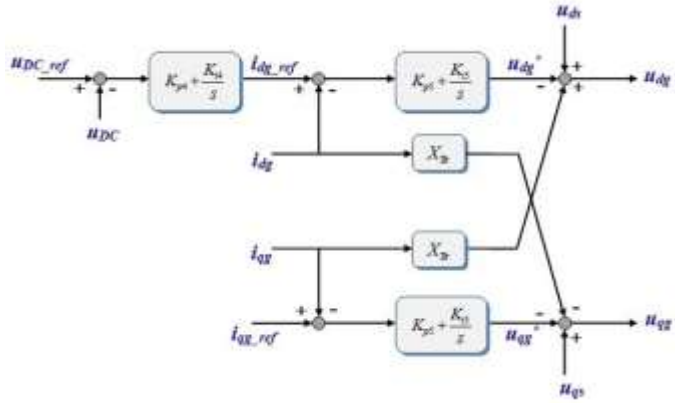

Figure 4. Block diagram of Grid Side Converter controller

$$\frac{dx_5}{dt} = u_{DC\_ref} - u_{DC} \tag{14}$$

$$\frac{dx_6}{dt} = -K_{p4}\Delta u_{DC} + K_{i4}x_5 - i_{dg} \tag{15}$$

$$\frac{dx_7}{dt} = i_{qg\_ref} - i_{qg} \tag{16}$$

Parameters;

x_5 x_6 x_7 → Intermediate variables

K_{p4} K_{i4} → DC bus voltage regulator gains

K_{p5} K_{i5} → GSC converter current regulator gains

u_{DC_ref} → Reference voltage of DC Link

3. Tuning of PI Controller Parameters using SaDE

Objective Function Formulation:

The main objective of this paper is to tune the parameters K_{p1}, K_{i1}, K_{p2}, K_{i2}, K_{p3}, K_{i3}, K_{p4}, K_{i4}, K_{p5} and K_{i5} so that active power and terminal voltage tracks the reference values. So the objective function is formulated in such a way that

i. Active power error reduces to zero after a disturbance
ii. Terminal voltage error reduces with in short time.
iii. The change in DC bus voltage is very small.

To achieve the above mentioned integral square error[19] is adopted in this paper.

$$ISE = \int error^2\, dt$$

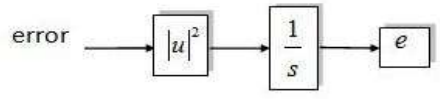

Figure 5. Representation of Integral square error

Now the objective function is,

$$\mathbb{F} = w_1 e_1 + w_2 e_2 + w_3 e_3 \quad (17)$$

Where,

e_1 is the active power integral square error

e_2 is the terminal voltage integral square error

e_3 is dc bus voltage integral square error

w_1, w_2, w_3 are the weight adjustments according to their priorities.

The selection of weights plays an important role in tuning the controllers. A wrong selection may lead the search to local minima. Based on the working of DFIG under various operating conditions, the following observations are made. Active power error falls is the range of 0.05 to 0.2 p.u. Terminal voltage error is in the range of 0.2 to 0.4 p.u. DC bus voltage error is the range of 50-150V. Thus there is a need to normalize the errors. There fore higher weightage is allotted for active power error and terminal voltage error and a low weightage for DC bus voltage error with $w_1 = 10, w_2 = 3, w_3 = 10^{-2}$.

The model of WT using DFIG is a high dimensional time varying system where the control parameters are to be tuned by using this SaDE algorithm. This SaDE Algorithm is developed for control parameter adaptation scheme with trial vector generation strategy. The algorithm of SaDE is given below.

A. Initialization:

There are 10 parameters to tune. For these parameters we have to assign the lower and upper bounds X_{min} & X_{max} according to actual control parameters.

Dimension of the problem is (D) = 10;

Initiate population (or) solution count (N_P) = 50;

Initializing bounds = $\begin{bmatrix} lower & bounds \\ upper & bounds \end{bmatrix}$

$$= \begin{bmatrix} 0.4 & 50 & 0.1 & 5 & 0.5 & 100 & 0.005 & 0.005 & 0.2 & 50 \\ 20 & 150 & 15 & 60 & 20 & 600 & 0.2 & 1 & 10 & 300 \end{bmatrix}$$

Here, lower & upper bounds for K_{p1}(=1) are taken as 0.4 & 20 respectively.

The mean of cross-over rate C_R is initialized to 0.5 and learning period generation to 50. Four mutation strategies which are popular in literature are employed.

B. Evaluate best member after initialization:

Calculate the objective function from (17) for the initial 50 solutions (pop) in the first run and arrive best member.

C. Selection of mutation strategy:

Selection of a suitable mutation strategy for given problem is highly tedious job and requires rigorous simulations. SaDE algorithm adopts the suitable approach based on the success rate in the past. One mutation approach is randomly selected for the target vector. Objective function values are calculated from (17) for the new generated trial vectors. Success and failure rate for each mutation strategy is recorded based on the number of trial vectors that results in new solutions (population).For next generations, selection of mutation strategy for a given target vector will be decided based on the success rate of the previous generations.

D. Update Scaling Factor and Crossover:

The performance of DE is greatly influenced by control parameter C_R value. A wrong choice of C_R value will deteriorate the functioning of DE. Thus is a need to adopt the C_R value. A set of parameter C_R values with a mean of 0.5 is randomly selected and applied to target vectors.

Optimum C_R values are recorded based on the success of trial vectors that accounts for new population. A set of α values are randomly selected.

E. Terminating conditions:

The search criteria terminates when the stopping conditions are satisfied. In this paper, the search condition terminates when the evaluations (η) are greater than Max-Gen.

The flowchart of SaDE algorithm is shown in Figure 6.

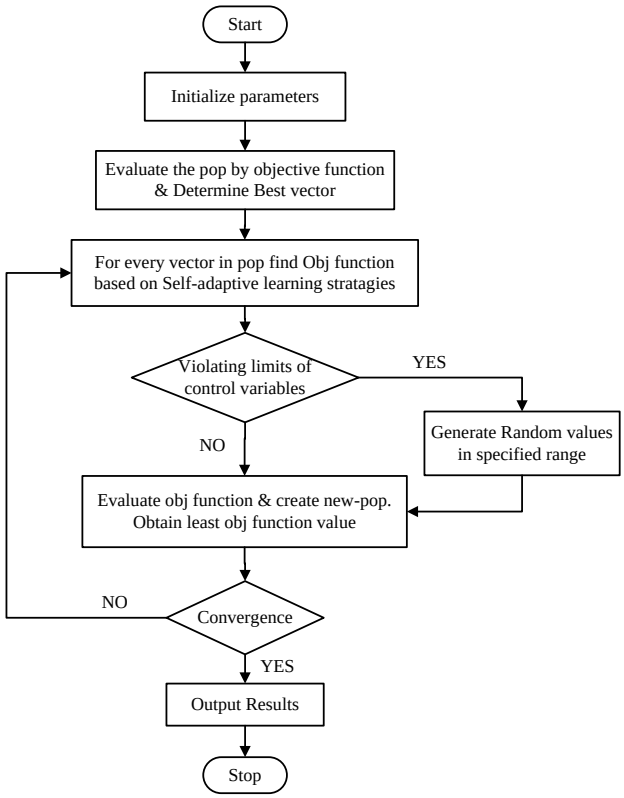

Figure 6. SaDE Flow chart

4. Simulation Results

A 9 MW wind farm with six 1.5 MW wind turbines is considered for study in this paper. The complete details of this model are given in MATLAB demos. The Single line diagram of wind energy system is shown in Figure 7. The parameters are tuned using SaDE algorithm which has been written in m-file that calls the Simulink file for all the iterations. In simulations the below 7 cases are studied:

i. Fault simulated at middle of the line in Super-synchronous mode.
ii. Fault simulated at middle of the line in Synchronous mode.
iii. Fault simulated at middle of the line in Sub-synchronous mode.
iv. Fault simulated at 10 km away from the generator in Super-synchronous mode.
v. Fault simulated at 10 km away from the generator in Synchronous mode.
vi. Fault simulated at 10 km away from the generator in Sub-synchronous mode.
vii. A sudden change in reference terminal voltage.

Finally control parameters are modified by using SaDE technique and observed the results of terminal voltage, DC link voltage, active and reactive powers. In all simulations the voltage of DC link is maintained constant at 1200 V.

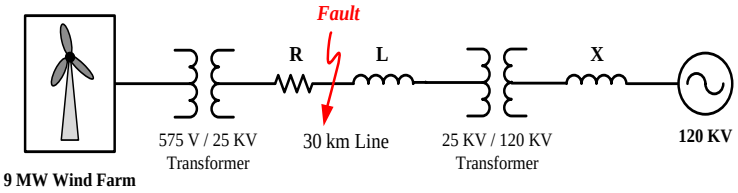

Figure 7. Single line diagram of WT using DFIG

Tuned parameters of the controllers using SaDE are presented in Table 1. The parameters obtained without optimization are obtained from [22]. Elapsed time for tuning these 10 control parameters is 5,243.75s. Based on the obtained values the simulations are carried.

Table 1. Without optimization and SaDE parameters of controllers

Parameters	K_{p1}	K_{i1}	K_{p2}	K_{i2}	K_{p3}	K_{i3}	K_{p4}	K_{i4}	K_{p5}	K_{i5}
Without Optimization	1	100	0.3	8	1.25	300	0.002	0.05	1	100
SaDE	2.39	85.21	4.93	43.25	5.53	356.41	0.0098	0.295	7.77	156.70

Case 1: At Super-synchronous mode, when fault is simulated at middle of the line

A symmetrical fault (3-phase to ground) is applied at middle of the 30 km transmission line for 9 cycles during the time interval of 50s to (50+9/60)s with a fault resistance of 20Ω. Based on the wind speed $(V_\omega = 12 m/s)$ power generation is of 6.45 MW and DFIG is operating in Super-synchronous mode of operation with the rotor speed of 1.2 pu.

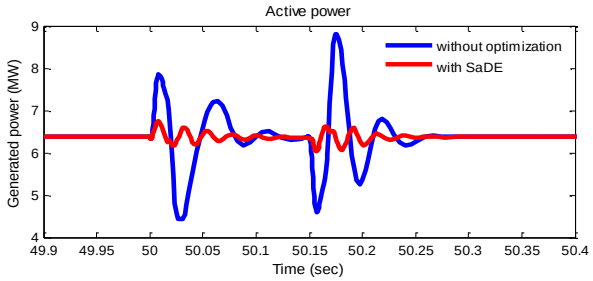

Figure 8. Active power with fault on mid-point at V_ω =12 m/s

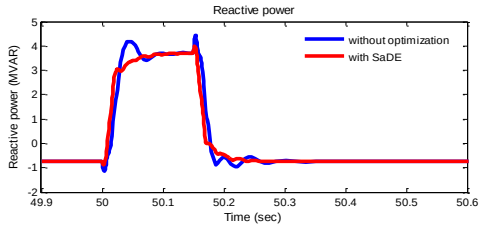

Figure 9. Reactive power with fault on mid-point at V_ω =12 m/s

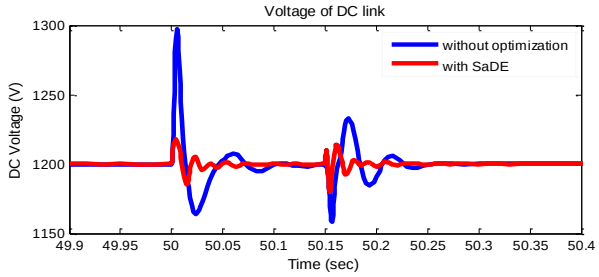

Figure 10. Voltage of DC link with fault on mid-point at V_ω =12 m/s

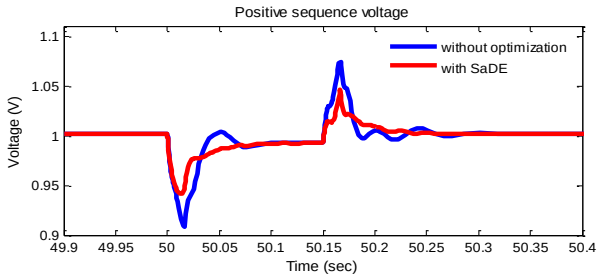

Figure 11. Terminal voltage with fault on mid-point at V_ω =12 m/s

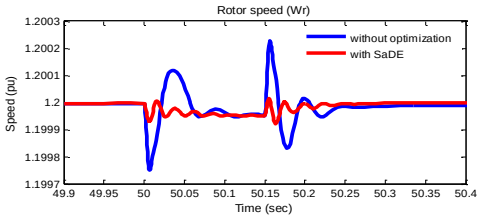

Figure 12. Rotor speed with fault on mid-point at V_ω =12 m/s

Simulation results of Active power, Reactive power, Voltage of DC link, Terminal voltage and Rotor speed are shown in Figure 8-12. In all these results SaDE tuned system is compared with the actual system. With SaDE tuned parameters peak value of active power is 6.7 MW which is lower when compared to actual system with peak value of 7.9 MW. Similarly undershoot value of 6.1 MW in active power is lower when compared to actual system with undershoot value of 4.4 MW with drastic change. Terminal voltage profile of the generator is improved when compared to actual system with less overshoot. The settling time with SaDE parameters is less when compared to actual system and hence system response is fast. Peak value of DC link voltage is reduced. The speed oscillation on the rotor gets reduced. Therefore we can conclude that the overall response of the system is improved.

Case 2: At Synchronous mode, when fault is simulated at middle of the line

A symmetrical fault is applied at middle of the 30 km transmission line for 9 cycles with the fault resistance of 20Ω as in the above case. Based on the wind speed $(V_\omega = 10\,m/\mathrm{s})$ the power generation is 3.6 MW and DFIG operates in Synchronous mode with the rotor speed of 1.0 pu with slip zero. Simulation results are shown in Figure 13-17. Results with SaDE technique are compared with actual parameters of the system.

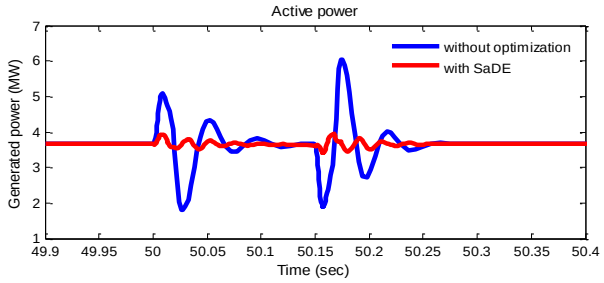

Figure 13. Active power with fault on mid-point at V_{ω} =10 m/s

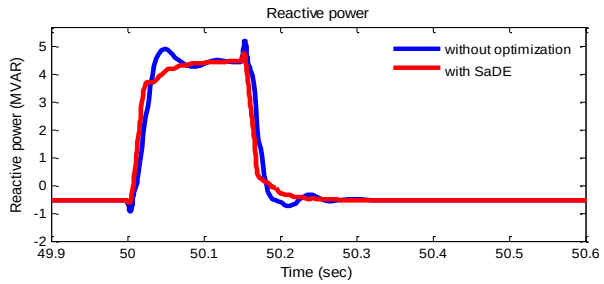

Figure 14. Reactive power with fault on mid-point at V_{ω} =10 m/s

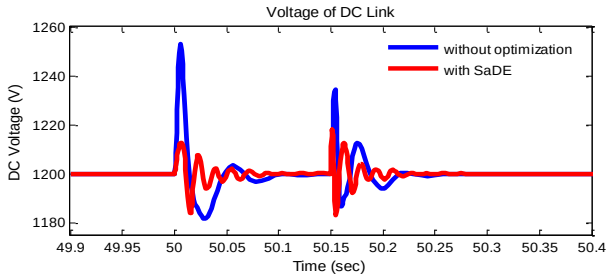

Figure 15. Voltage of DC link with fault on mid-point at V_{ω} =10 m/s

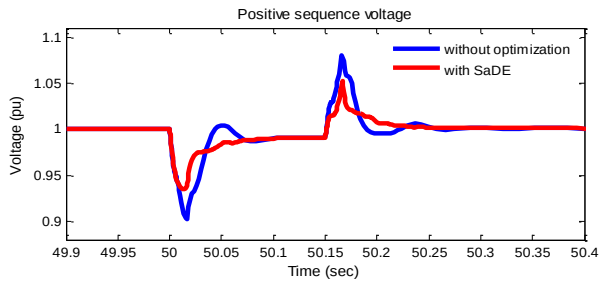

Figure 16. Terminal voltage with fault on mid-point at V_{ω} =10 m/s

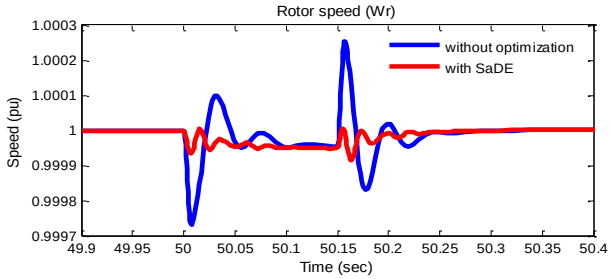

Figure 17. Rotor speed with fault on mid-point at V_{ω} =10 m/s

By observing results with optimized parameters peak value is 3.9 MW which is lower compared to actual system with peak value of 5.15 MW. Similarly undershoot value of 3.5 MW in active power is lower when compared to actual system with undershoot value of 1.75 MW and settling time of the system is 50.26 which gets reduced compared with actual system. DC link voltage shoots is reduced but oscillations are high because less weightage is given to DC bus voltage error.

Case 3: At Sub-synchronous mode, when fault is simulated at middle of the line

At middle of the line a symmetrical fault is applied for 9 cycles with the fault resistance of 20Ω as in the *Case 1*. With the low wind speed $(V_{\omega} = 8 m/\sec)$ generating power is 1.9 MW and DFIG operates in Sub-synchronous mode with the rotor speed of 0.8 pu with slip 0.2. Simulation results are shown in Figure 18-22. By observing active power with optimized parameters peak overshoot value is 2 MW which is lower compared to actual system with peak value of 3.3 MW. Similarly undershoot value of 1.8 MW is lower when compared to actual system with undershoot value of 0.2 MW. DC link voltage oscillations are high because less weightage is given.

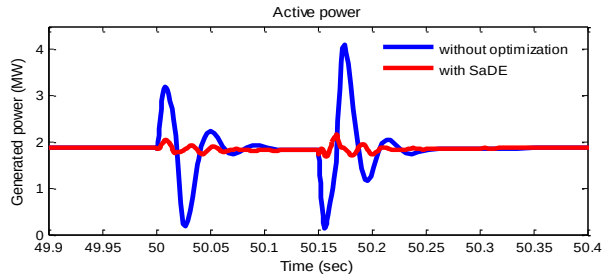

Figure 18. Active power with fault on mid-point at V_{ω} =8 m/s

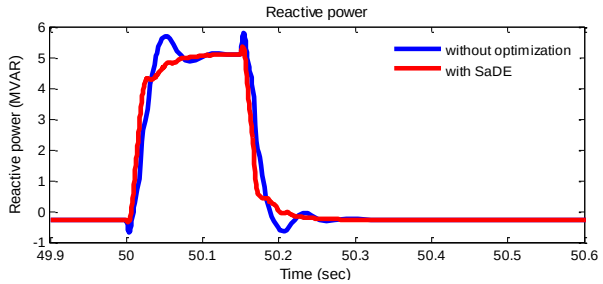

Figure 19. Reactive power with fault on mid-point at V_{ω} =8 m/s

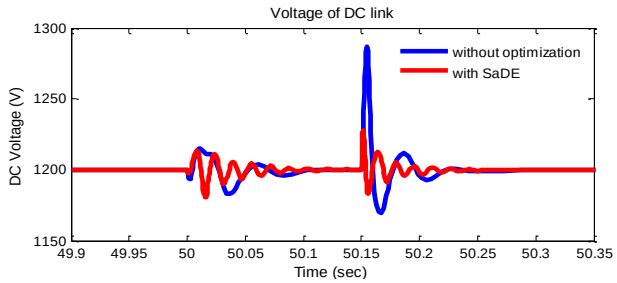

Figure 20. Voltage of DC link with fault on mid-point at V_{ω} =8 m/s

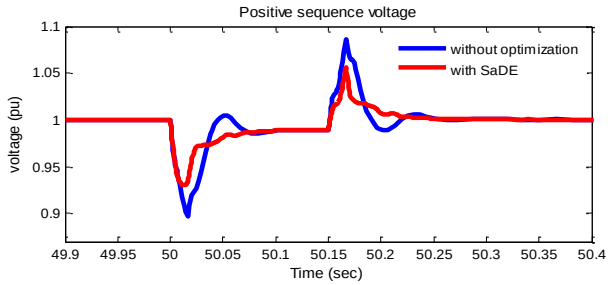

Figure 21. Terminal voltage with fault on mid-point at V_{ω} =8 m/s

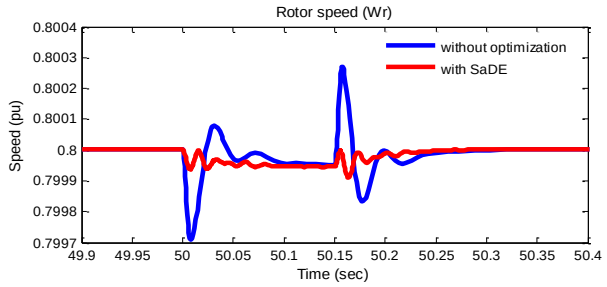

Figure 22. Rotor speed with fault on mid-point at V_{ω} =8 m/s

Case 4: At Super-synchronous mode, when fault is simulated at 10 km away from the generator

A symmetrical fault is applied to the transmission line on 10 km away from the system for 9 cycles with a fault resistance of 20Ω. Based on the wind speed $(V_{\omega} = 12\,m/s)$ DFIG operates in Super-synchronous mode with the rotor speed of 1.2 pu with slip -0.2. Simulation results for Active power, Reactive power, Voltage of DC link, Terminal voltage and Rotor speed are shown in Figure 23-27. With optimized parameters peak overshoot value is 6.2 MW which is lower compared to actual system with peak value of 8 MW. Similarly undershoot value of -0.1 MW in active power is lower when compared to actual system with undershoot value of -3MW.

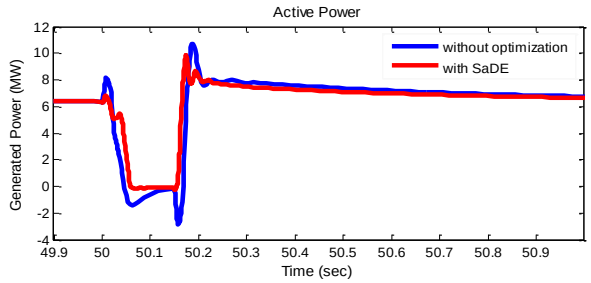

Figure 23. Active power with fault is at 10 km away from system at V_{ω} =12 m/s.

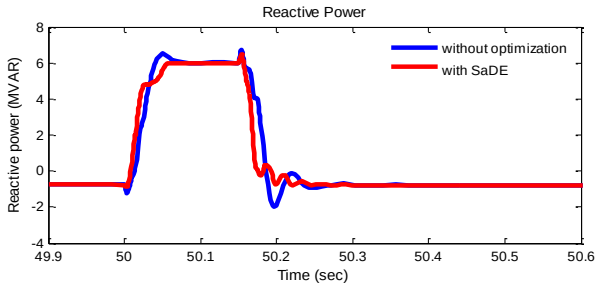

Figure 24. Reactive power with fault is at 10 km away from system at V_{ω} =12 m/s

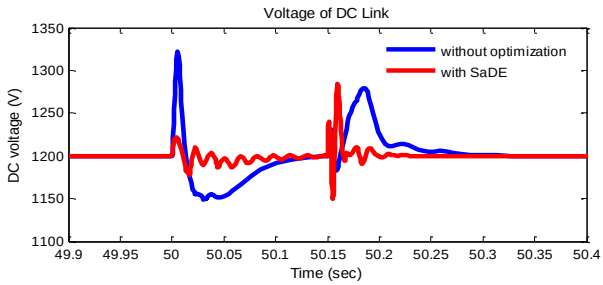

Figure 25. Voltage of DC link with fault is at 10 km away from system at V_{ω} =12 m/s

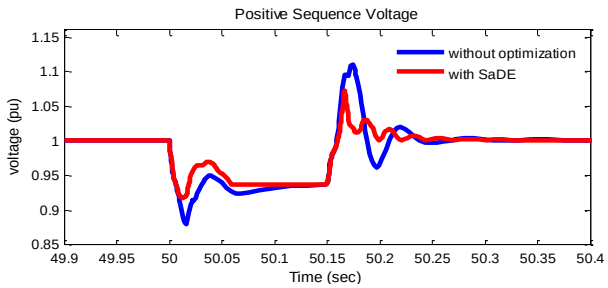

Figure 26. Terminal voltage with fault is at 10 km away from system at V_{ω} =12 m/s

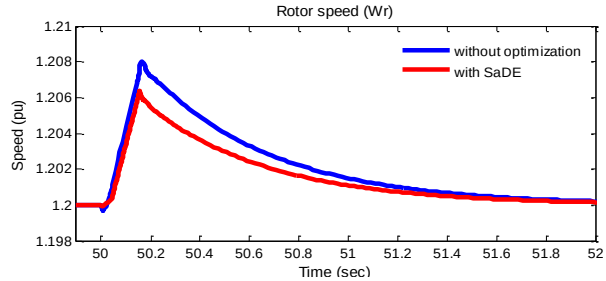

Figure 27. Rotor speed with fault is at 10 km away from system at V_{ω} =12 m/s.

Terminal voltage profile of the generator is improved when compared to actual system with less overshoot. The settling time with SaDE parameters is less when compared to actual system and hence system response is fast along with the rotor speed and settling time of the terminal voltage is 0.3 s. Peak value of DC link voltage is reduced but oscillations increases due to less priority for DC voltage weight adjustment.

Case 5: At Synchronous mode, when fault is simulated at 10 km away from the generator

A symmetrical fault is applied to the transmission line on 10 km away from the system for 9 cycles with the fault resistance of 20Ω as in the above case. Based on the wind speed $(V_{\omega} = 10\,m/\mathrm{s})$ DFIG is operating in Synchronous mode with the rotor speed of 1.0pu with slip zero. Simulation results are shown in Figure 28-32. Results with SaDE technique are compared with actual parameters of the system.

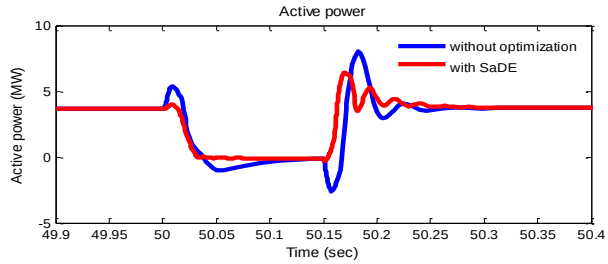

Figure 28. Active power with fault is at 10 km away from system at V_{ω} =10 m/s

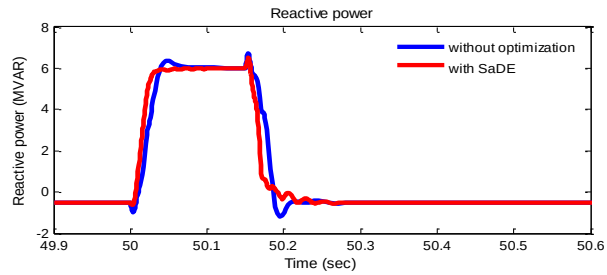

Figure 29. Reactive power with fault is at 10 km away from system at V_{ω} =10 m/s

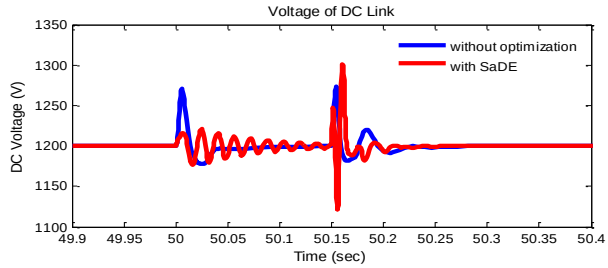

Figure 30. Voltage of DC link with fault is at 10 km away from system at V_{ω} =10 m/s

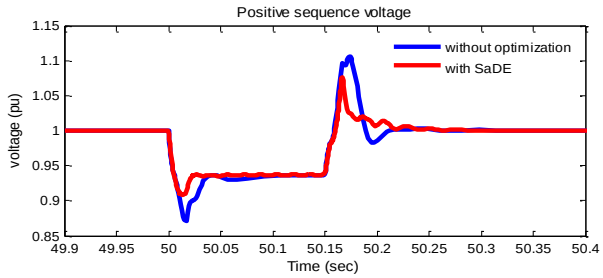

Figure 31. Terminal voltage with fault is at 10 km away from system at V_ω =10 m/s

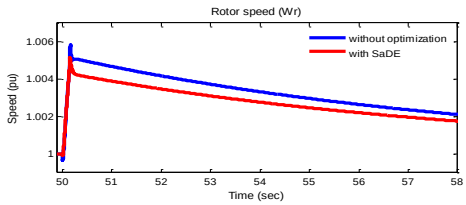

Figure 32. Rotor speed with fault is at 10 km away from system at V_ω =10 m/s.

By observing results with optimized parameters peak value of 4 MW which is lower compared to actual system with peak value of 5.7 MW. Similarly undershoot value of 0.1 MW in active power is lower when compared to actual system with undershoot value of 2.8MW and settling time is reduced compared with actual system. But the DC link voltage is similar to actual system because less weightage is given to DC bus voltage error. Rotor speed settles quickly with tuned parameters compared with actual once.

Case 6: At Sub-synchronous mode, when fault is simulated at 10 km away from the generator

At 10 km away from the system a symmetrical fault is applied to the transmission line for 9 cycles with the fault resistance of 20Ω as in the above case 4. Based on the wind speed $(V_\omega = 8 m/\sec)$ DFIG is operating in Sub-synchronous mode with the rotor speed of 0.8 pu. Simulation results are shown in Figure 33-37. Results with SaDE technique are compared with actual parameters of the system. Active power of the system with optimized parameters the peak overshoot is lower compared to actual system and settling time is also reduced. Transients of the Reactive power and terminal voltage are improved. But the DC link voltage is similar to actual system because less weightage is given to DC bus voltage error. Rotor speed settles quickly with tuned parameters compared with actual once.

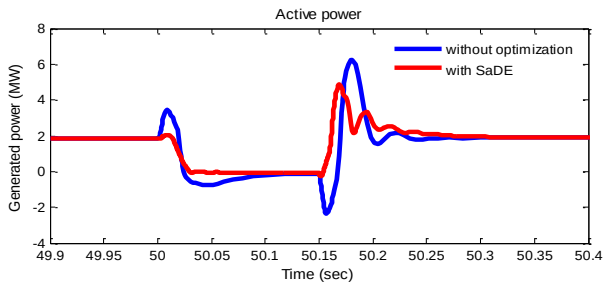

Figure 33 Active power with fault is at 10 km away from system at V_ω = 8 m/s

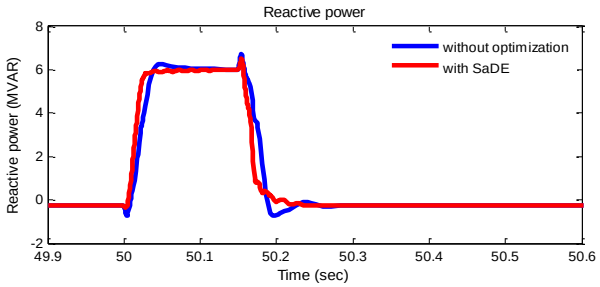

Figure 34. Reactive power with fault is at 10 km away from system at V_ω = 8 m/s

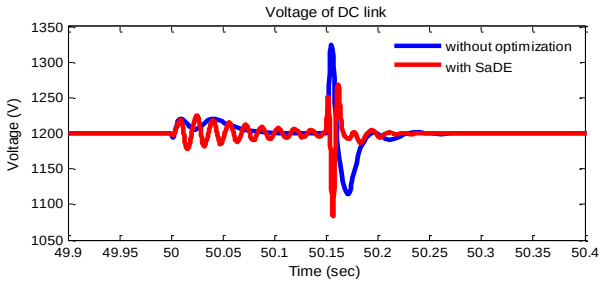

Figure 35. Voltage of DC link with fault is at 10 km away from system at V_ω = 8 m/s

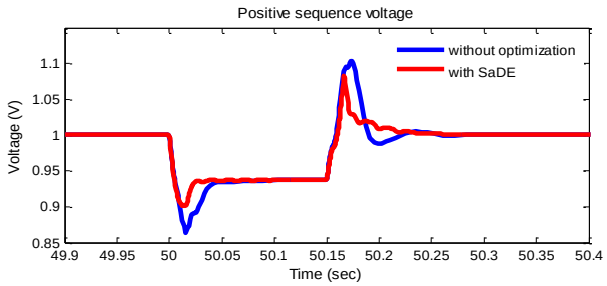

Figure 36. Terminal voltage with fault is at 10 km away from system at V_ω = 8 m/s

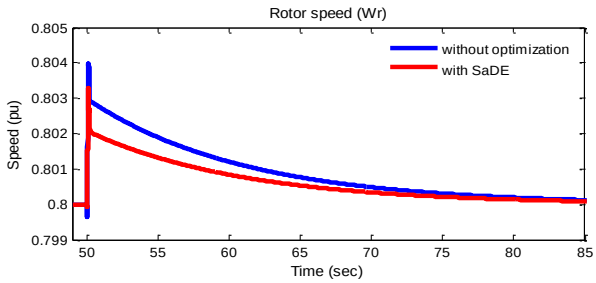

Figure 37. Rotor speed with fault is at 10 km away from system at V_ω = 8 m/s.

Case 7: When reference voltage of DFIG is reduced from 1.0 pu to 0.9 pu

At sudden change in Reference voltage of DFIG from 1.0 pu to 0.9 pu at fault less line with the wind speed of $V_\omega = 12\,m/s$ at slip -0.2 operates under Super-synchronous mode. Simulations of the five components are resulted and are shown in Figure 38-42. Results for active power with optimized parameters peak value of 4 MW which is lower compared to actual system with peak value of 5.7 MW. Similarly undershoot value of 0.1 MW is lower compared to actual system with undershoot value of 2.8MW. Shoots of the DC link voltage is reduced. Hence simulation results for sudden change in reference voltage and different fault locations with various modes

of operation proves the performance of the system gets improved by observing objective functions, settling time, peak overshoot and undershoots with minimized errors.

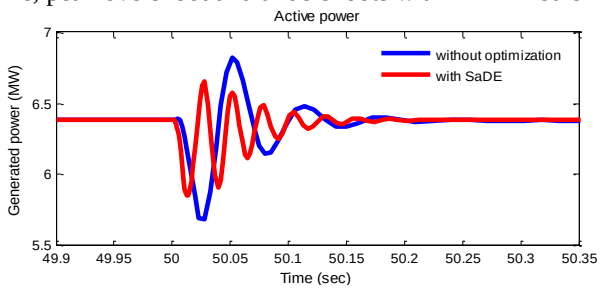

Figure 38. Active power with reduced reference voltage

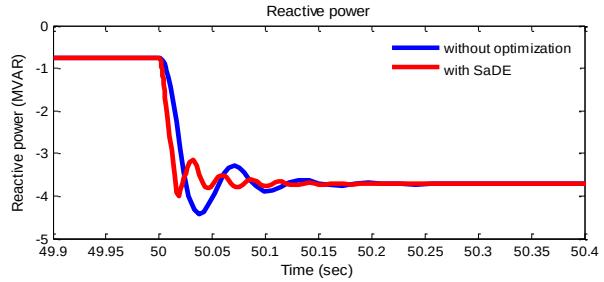

Figure 39. Reactive power with reduced reference voltage

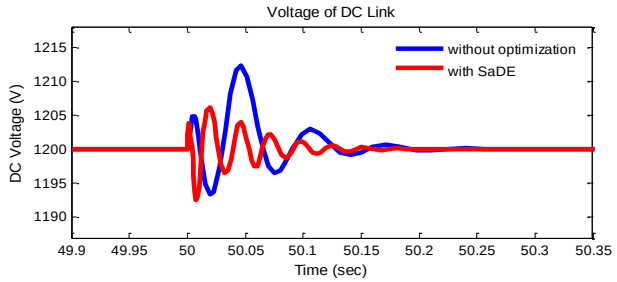

Figure 40. Voltage of DC link with reduced reference voltage

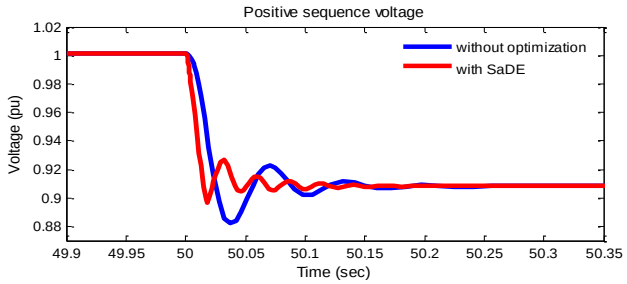

Figure 41. Terminal voltage with reduced reference voltage

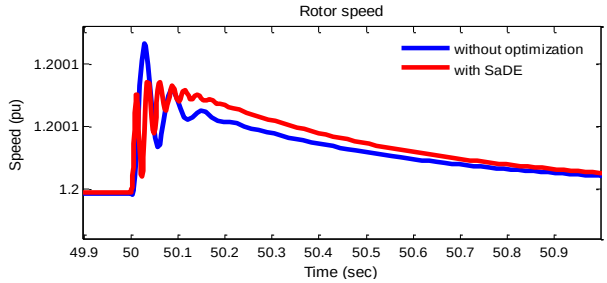

Figure 42. Rotor speed with reduced reference voltage

Therefore we can conclude that the overall response of the system is improved.

Here Table 2 and Table 3 shows the objective function values at different wind speeds with actual and optimized parameters for three-phase fault induced at the middle of the line and 10km away from the wind system. The objective function value is very low for SaDE tuned system when compared to actual system.

Table 2. Objective function value when fault is at middle of the line

Wind speed	***Actual***	***PSO***	***SaDE***
$V_\omega = 12 m/\text{s}$ (Super-synchronous)	4.7356	2.7375	0.2026
$V_\omega = 10 m/\text{s}$ (Synchronous)	3.3987	1.7875	0.1083
$V_\omega = 8 m/\text{s}$ (Sub-synchronous)	3.1348	1.2863	0.1379

Table 3. Objective function value when fault is 10 km away from system

Wind speed	***Actual***	***PSO***	***SaDE***
$V_\omega = 12 m/\text{s}$ (Super-synchronous)	7.9158	3.6279	1.1045
$V_\omega = 10 m/\text{s}$ (Synchronous)	4.0239	2.0538	0.8909
$V_\omega = 8 m/\text{s}$ (Sub-synchronous)	4.4091	1.4461	0.7812

5. Conclusion

This paper proposed the tuning of 10 control parameters at-a-time by Self-adaptive Differential Evolution algorithm. This approach adopts the generation of trail vector strategies and their respective control parameter values are self adopted by its own analysis based on the previous experiments with promising values. Vector control of wind system with DFIG is obtained by the dynamic model equations. Simulation studies are carried on 9 MW wind farm with sudden change in reference voltage, three-phase faults induced at middle of the line and 10 km away from the wind system with various modes like Super-synchronous, Synchronous and Sub-synchronous modes. The evaluated parameters of the PI controller gives better results when compared with the actual existed system control parameters. The results shows that the performance and stability of the system is improved in terms of settling time, peak overshoot and undershoot. Hence, overall response of the system is improved. This work can be extended by applying this technique to handle the load harmonics.

6. References

[1]. http://www.windustry.org

[2]. Parida A, Chatterjee D (2016) An improved control scheme for grid connected doubly fed induction generator considering wind-solar hybrid system. *Int J Electr Power Energy Syst* 77:112–122. doi: 10.1016/j.ijepes.2015.11.036

[3]. Aktarujjaman M, Haque ME, Muttaqi KM, et al. (2008) Control Dynamics of a doubly fed induction generator under sub- and super-synchronous modes of operation. In: 2008 IEEE Power Energy Soc. Gen. Meet. - Convers. Deliv. *Electr. Energy 21st Century. IEEE*, pp 1–9

[4]. Kerrouche K, Mezouar A, Belgacem K (2013) Decoupled control of doubly fed induction generator by vector control for wind energy conversion system. *Energy Procedia* 42:239–248. doi: 10.1016/j.egypro.2013.11.024

[5]. Kairous D, Wamkeue R (2011) Sliding-mode control approach for direct power control of WECS based DFIGURE 2011 10th *Int Conf Environ Electr Eng EEEICEU* 2011 - Conf Proc 1–4. doi: 10.1109/EEEIC.2011.5874836

[6]. Karthikeyan A, Naguru NR, Nagamani C, Ilango GS (2011) Feedback Linearization control based power control of grid connected DFIG with grid synchronization. 2011 10th Int Conf Environ Electr Eng 1–4. doi: 10.1109/EEEIC.2011.5874757

[7]. Feng Wu, Xiao-Ping Zhang, Ping Ju, Sterling MJH (2008) Decentralized Nonlinear Control of Wind Turbine With Doubly Fed Induction Generator. *IEEE Trans Power Syst* 23:613–621. doi: 10.1109/TPWRS.2008.920073

[8]. Gude JJ, Kahoraho E (2010) Modified Ziegler-Nichols method for fractional PI controllers. *Proc 15th IEEE Int Conf Emerg Technol Fact Autom ETFA* 2010 0–4. doi: 10.1109/ETFA.2010.5641074

[9]. Gude JJ, Kahoraho E (2012) Kappa-tau type PI tuning rules for specified robust levels. *IFAC Proc Vol 2:589–594. doi: 10.1109/ETFA*.2012.6489612

[10]. Storn R, Price K (1997) Differential evolution–a simple and efficient heuristic for global optimization over continuous spaces. *J Glob Optim* 11:341–359. doi: 10.1023/A:1008202821328

[11]. Bolognani S, Oboe R, Zigliotto M (1999) Sensorless full-digital PMSM drive with EKF estimation of speed and rotor position. *IEEE Trans Ind Electron* 46:184–191. doi: 10.1109/41.744410

[12]. Das S, Abraham A, Chakraborty UK, Konar A (2009) Differential evolution using a neighborhood-based mutation operator. *IEEE Trans Evol Comput* 13:526–553. doi: 10.1109/TEVC.2008.2009457

[13]. Wang Y, Cai Z, Zhang Q (2011) Differential evolution with composite trial vector generation strategies and control parameters. *IEEE Trans Evol Comput* 15:55–66. doi: 10.1109/TEVC.2010.2087271

[14]. Qin AK, Huang VL, Suganthan PN (2009) Differential evolution algorithm with strategy adaptation for global numerical optimization. *IEEE Trans Evol Comput* 13:398–417. doi: 10.1109/TEVC.2008.927706

[15]. Tang Y, Ju P, He H, et al. (2013) Optimized control of DFIG-based wind generation using sensitivity analysis and particle swarm optimization. *IEEE Trans Smart Grid* 4:509–520. doi: 10.1109/TSG.2013.2237795

[16]. Oliveira PS, Barros LS, de Q Silveira LG (2010) Genetic algorithm applied to state feedback control design. Transm Distrib Conf Expo Lat Am (T&D-LA), *2010 IEEE/PES 480–485. doi: 10.1109/TDC-LA*.2010.5762925

[17]. Brest J, Bošković B, Greiner S, et al. (2007) Performance comparison of self-adaptive and adaptive differential evolution algorithms. Soft Comput 11:617–629. doi: 10.1007/s00500-006-0124-0

[18]. Mishra Y, Mishra S, Li F (2012) Coordinated tuning of DFIG-based wind turbines and batteries using bacteria foraging technique for maintaining constant grid power output. *IEEE Syst* J 6:16–26. doi: 10.1109/JSYST.2011.2162795

[19]. Sharaf AM, El-Gammal AAA (2009) An Integral Squared Error -ISE optimal parameters tuning of modified PID controller for industrial PMDC motor based on Particle Swarm Optimization-PSO. 2009 *IEEE 6th Int Power Electron Motion Control Conf IPEMC* '09 1953–1959. doi: 10.1109/IPEMC.2009.5157716

[20]. The Mathworks Inc., MATLAB/SimPowerSystemsDemos/ Wind FarmPhasormodel.

Hemanth KR Alluri received B.Tech degree in Electrical & Electronics Engineering from JNTU Kakinada, Andhra Pradesh, India and received his M.Tech degree in Power & Industrial Drives from GMR Institute of Technology, Rajam, India. Currently he is working as Assistant professor in Department of Electrical and Electronics Engineering, SRKR Engineering College, India. His research interests on Renewable energies, Multilevel Inverters, Optimization Techniques and Power Quality.

Ayyarao S.L.V. TUMMALA received B.Tech and M.Tech in electrical and electronics engineering from JNTU, Andhra Pradesh. He is pursuing his Ph.D. in ANU, India. He is presently working as assistant professor in Department of Electrical and Electronics Engineering, GMR Institute of Technology, Rajam. His research interests are application of optimization techniques of conventional PID and fractional order PID and intelligent-based controller.

Ramanarao PV is working as professor and head of department in Electrical and Electronics Engineering in University College of Engineering, ANU, Guntur. He has guided several research scholars in diverse fields of power systems. His research interests include power system stabilizers, DFIG controller for wind power generation, Wavelet-based protection of power system, Application

PVN Mohan Krishna received B. E degree in Electrical & Electronics Engineering from S.R.K.R Engineering College (Affiliated to Andhra University), Andhra Pradesh, India and received his M.Tech degree in Power Systems from National Institute of Technology, Warangal, India. He currently working towards his Ph.D. in Indian Institute of Technology, Bhubaneswar, India. His research interests includes Renewable energy systems, Optimal Planning and control of Hybrid microgrids, data analytics and optimization applied to power system.